Oxidative Stress, Neuroinflammation, and Neuronal Vulnerability Begin in Midlife: a 7 Tesla Magnetic Resonance Spectroscopy Healthy Adult Lifespan Study

Flavie E. Detcheverry[1,2,3], Sneha Senthil[4,5], Rozalia Arnaoutelis[4,5], Samson Antel[4,5], Haz-Edine Assemlal[5,6], Zahra Karimaghaloo[6], Douglas L. Arnold[4,5], Jamie Near[7,8], Sridar Narayanan[4,5 *], AmanPreet Badhwar[1,2,3 *]

[1]Multiomics Investigation of Neurodegenerative Diseases (MIND) lab, Centre de Recherche de l'Institut Universitaire de Gériatrie de Montréal (CRIUGM), 4545 Chemin Queen May, Montréal, QC, H3W 1W4, Canada;

[2]Department of Pharmacology and Physiology, Faculty of Medicine, University of Montreal, 2900 Boulevard Édouard-Montpetit, Montréal, QC, H3T 1J4, Canada;

[3]Institute of Biomedical Engineering, University of Montreal, 2960 Chemin de la Tour, Montréal, QC, H3T 1J4, Canada;

[4]Department of Neurology and Neurosurgery, Faculty of Medicine and Health Sciences, McGill University, 1033 Pine Avenue West, Montréal, QC, H3A 1A1, Canada;

[5]McConnell Brain Imaging Centre, Montreal Neurological Institute-Hospital, 3801 University Street, Montréal, QC, H3A 2B4, Canada;

[6]NeuroRx Research, a Clario Company, 3575 Parc Avenue, Suite #5322 Montréal, QC, H2X 3P9, Canada;

[7]Physical Sciences, Sunnybrook Research Institute, 2075 Bayview Avenue, Toronto, ON, M4N 3M5, Canada;

[8]Department of Medical Biophysics, Faculty of Medicine, University of Toronto, 101 College Street, Toronto, ON, M5G 1L7, Canada.

[*] Co-senior authorship

Correspondence

AmanPreet Badhwar, MSc, PhD

Multiomics Investigation of Neurodegenerative Diseases (MIND) lab, Centre de Recherche de l'Institut Universitaire de Gériatrie de Montréal (CRIUGM)

4545 Chemin Queen May, Montréal, QC, H3W 1W4, Canada

Email: amanpreet.badhwar@umontreal.ca

Telephone: 001 (514) 340-3540, extension 3345

Sridar Narayanan, PhD

McConnell Brain Imaging Centre, Montreal Neurological Institute-Hospital

Department of Neurology and Neurosurgery, McGill University

3801 University Street, WM 321, Montréal, QC, H3A 2B4, Canada

Email: sridar.narayanan@mcgill.ca

Telephone: 514-398-8258

ABSTRACT

INTRODUCTION: While changes associated with age-related diseases, like oxidative stress, begin in midlife, most aging studies focused on older individuals. Our study assessed *in vivo* brain metabolites in healthy adults, including the understudied middle-age group.

METHODS: 7 tesla magnetic resonance spectroscopy data were acquired from 95 healthy adults (48 women) aged 20-79 years. Eight metabolites were measured in posterior cingulate cortex (PCC) and centrum semiovale white matter (CSWM).

RESULTS: With increasing age, we found (a) lower glutathione and glutamate, and higher *myo*-inositol in PCC, and (b) lower *N*-acetylaspartate and glutamate, and higher *myo*-inositol, total creatine, and *N*-acetylaspartyl-glutamate in CSWM. Notably, most changes started in midlife and were driven by age-related changes in women.

DISCUSSION: Overall, we found evidence that oxidative stress, neuroinflammation, and neuronal vulnerability begin in midlife in healthy adults. Targeting these processes in midlife may slow brain aging and reduce age-related neurodegenerative diseases risk, including Alzheimer's disease.

GRAPHICAL ABSTRACT

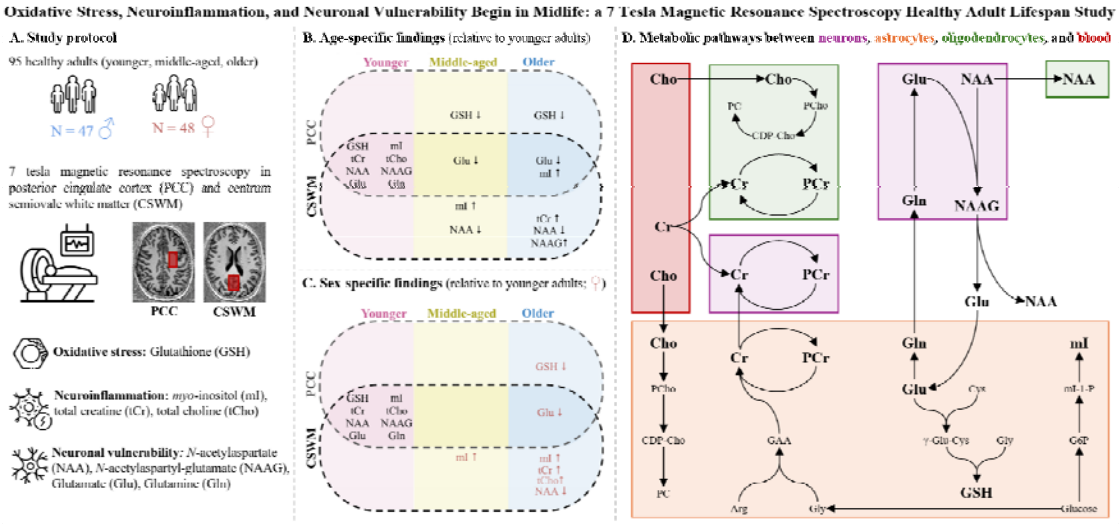

1. INTRODUCTION

Higher life expectancy is accompanied by higher prevalence of age-related neurodegenerative diseases (NDDs), with Alzheimer's disease (AD) being the most prevalent [1]. Evidence suggests that NDD-associated structural, functional, and molecular brain changes begin in midlife (40+ years) [2,3], and might be accelerated by menopause in women [2]. Therefore, the transition from middle- to older-age is crucial for future health and might offer a window for cognitive decline prevention. Notably, the 2024 *Lancet's* Commission on Dementia reported that addressing 14 identified risk factors could prevent 45% of dementia cases, with ten, including metabolic health, occurring in midlife and potentially reducing dementia risk by 30% [4]. Despite this, most aging- and NDD-studies focused on older individuals (60+ years).

Oxidative stress (OS) has been hypothesized as a key contributor to age-related decline [5,6]. OS results from an imbalance between the production and neutralization of reactive oxygen species (ROS), like hydrogen peroxide [7]. This imbalance is amplified in midlife as ROS accumulate, gradually weakening antioxidant defenses and disrupting homeostasis [8], with menopause further increasing oxidative stress in women [9]. Being the most energetically demanding organ [10], the brain, and especially hub regions like the posterior cingulate cortex (PCC) [11,12], are particularly vulnerable to OS. Antioxidants, with the most prevalent being the metabolite glutathione (GSH), can help neutralize ROS and protect against oxidative damage [6]. GSH and other metabolites can be assessed in the brain *in vivo* using magnetic resonance spectroscopy (MRS). GSH levels were found to (a) decrease with age in posterior regions in older relative to younger adults and in younger-to-middle-aged adults as one group, reflecting lower antioxidant capacity, and (b) increase in frontal regions

in older relative to younger adults, suggesting a compensatory mechanism against increased OS [7]. GSH differences with middle-aged healthy adults as a distinct group, however, have not been investigated with MRS.

In addition to GSH reflecting antioxidant capacity, additional metabolites can be assessed *in vivo* using MRS, reflecting neuroinflammatory and neurodegenerative processes. MRS-detected metabolites most studied include *N*-acetylaspartate (NAA; neuroaxonal marker); *N*-acetylaspartyl-glutamate (NAAG; neuromodulator); glutamate (Glu; main excitatory neurotransmitter); choline (Cho; membrane turnover marker); *myo*-inositol (mI; gliosis marker); and creatine (Cr; energy substrate) [13]. Although decreased NAA and Glu, and increased Cho, mI, and Cr levels have commonly been reported with increasing age, there lacks consensus [14–16], with variable ages and sample sizes across studies being a likely contributor. Specifically, studies investigating middle-aged healthy adults are lacking, an age group where changes enhancing risks of developing an NDD later in life are thought to appear [17,18].

Other reasons might explain the lack of consensus and increase the variability of MRS findings. Notably, the variety of MRS parameters and quantification techniques (e.g., ratios to Cr) can influence metabolite detection and complicate results interpretation. For example, using 1.5 tesla (T), McIntyre et al. reported higher total NAA and total Cr levels in centrum semiovale white matter (CSWM) using short echo time (TE), and no significance using long TE [19]. There is also a scarcity of 7T MRS studies, a magnet strength providing better signal-to-noise ratio, improved spectral resolution [20,21], and excellent reproducibility of low-concentration metabolites measurements like GSH [7,21]. Finally, most age-related metabolite findings are region-specific [7,22], which might be due to the underlying tissue

composition, as some metabolites are preferentially located in certain cell types (e.g., GSH in glia).

Therefore, we assessed brain metabolite level variations in healthy adults, including midlife, using 7T MRS in PCC and CSWM, two areas showing altered microstructure, metabolism, and connectivity in aging and NDDs (including AD) [11,12,23,24]. Given the increased sensitivity and specificity provided by ultra-high field (UHF) strength, ultra-short TE, and long repetition time (TR) [25], we were able to reliably measure levels of eight metabolites, including three low-concentration metabolites (GSH, NAAG, glutamine [Gln]). Specifically, we assessed the associations between metabolite levels and age, sex, and functional tests.

2. METHODS

2.1 Participants

Ninety-five healthy adults (48 women) belonging to three age groups were included: younger, 20-39 years, N = 32; middle-aged, 40-59 years, N = 32; older, 60-79 years, N = 31. Participants were recruited from the Montreal community using the word-of-mouth method, as well as from the *Banque de Participants* (https://criugm.qc.ca/la-recherche-jy-participe/conferences-de-la-banque-de-participants/) established at the *Centre de Recherche de l'Institut Universitaire de Gériatrie de Montréal* (CRIUGM). All participants were cognitively unimpaired and overall healthy. Exclusion criteria included cognitive complaint/worry, stroke, head trauma, psychiatric disorders, and magnetic resonance imaging (MRI)-related contraindications, such as metal in the body (e.g., pacemaker), claustrophobia, and pregnancy. Ethical approval was obtained from the aging-neuroimaging research ethics committee of the CIUSSS du *Centre-Sud-de-île-de-Montréal* (CIUSSS-CSMTL), and from the McGill University Institutional Review Board, Faculty of Medicine and Health Sciences. Written informed consent was obtained from all participants.

2.2 Functional Testing

Three measures sensitive to processing speed, manual dexterity, and gait/mobility were acquired, namely: (a) Processing Speed Test (PST) [26], based on the Symbol-Digit Modalities Test (SDMT), measuring processing speed, (b) the 9-hole Peg Test (9HPT), assessing manual dexterity, and (c) the Timed 25-foot Walk Test (T25FW) for gait and mobility. A description of each test has been provided in Supplementary Table S1.

2.3 MR Acquisition

In vivo brain data were acquired on a 7T Siemens Terra MR scanner at the McConnell Brain Imaging Centre of the Montreal Neurological Institute-Hospital (MNI; McGill University), using an 8-channel transmit and 32-channel receive head coil. T_1-weighted Magnetization-Prepared 2 Rapid Acquisition Gradient-Echo (MP2RAGE) images [27] were obtained for localization (TR/TE = 5000/2.33 ms; field of view (FOV): 240 mm; slice thickness = 0.70 mm; 1 average; 240 slices; acceleration factor = 3; acquisition time: 8 min 55 s). Using these anatomical images as reference, two MRS single-voxels were positioned (Fig. 1), one over the PCC/precuneus, a metabolically active hub region [11] (predominantly grey matter, GM), and the other over the CSWM, a region prone to age-related white matter damage [28] (predominantly white matter, WM). The PCC voxel (30 x 20 x 20 mm^3) was positioned at midline aligned posterior to the corpus callosum, and the CSWM voxel (30 x 15 x 15 mm^3) was placed in the left supraventricular WM. MRS spectra were acquired using the STimulated Echo Acquisition Mode (STEAM) sequence with the following parameters: TR/TE = 5000/8 ms; mixing time (TM) = 40 ms; flip angle = 90°; 64 to 96 averages in PCC, and 96 to 128 averages in CSWM; 4096 points; 5000 Hz spectral bandwidth; and acquisition time: 5 to 8 min in PCC, and 8 to 10 min in CSWM. Shimming was performed automatically using the Siemens "brain" B0 shim mode [29], and VAriable Power and Optimized Relaxations delays (VAPOR) method was used for water suppression [30]. Non-suppressed water spectra were acquired for eddy current correction and water reference quantification (TR/TE = 5000/8.00 ms; TM = 40 ms; 8 averages). Each scan lasted about 1 hour 15 minutes.

2.4 Image Processing and Analysis

T_1-weighted images were segmented into GM, WM, and cerebrospinal fluid (CSF) using the locally-developed Brain Tissue Composition-Net (BTCNet) pipeline, based on a published

framework [31]. Each MRS voxel was converted into a binary mask image in the T_1-weighted image space using another locally-developed software, built using the MINC Toolkit (https://bic-mni.github.io), and the fractions of the MRS voxel composed of GM, WM, and CSF were calculated.

2.5 Spectral Processing and Quantification

2.5.1 MRS Preprocessing and Processing

Raw MRS data was preprocessed using the FID Appliance (FID-A) [32] in Matlab (v2022b; MathWorks Inc. Natick, USA), before spectral fitting. Eddy current correction and spectral analysis were performed in LCModel (v6.3; Provencher Inc., Canada) [33], using a basis set consisting of 21 metabolite basis spectra and 9 macromolecule basis spectra. Specifically, the following metabolites were included in the basis set: alanine (Ala), aspartate (Asp), phosphocholine (PCh), creatine (Cr), phosphocreatine (PCr), gamma-aminobutyric acid (GABA), glutamine (Gln), glutamate (Glu), glutathione (GSH), glycine (Gly), *myo*-inositol (Ins), lactate (Lac), *N*-acetylaspartate (NAA), scyllo-inositol (Scyllo), taurine (Tau), glucose (Glc), *N*-acetylaspartyl-glutamate (NAAG), glycerophosphocholine (GPC), phosphatidylethanolamine (PE), serine (Ser), ascorbate (Asc), and nine macromolecule resonances (MM1-MM9). Macromolecular frequencies were: 0.89, 1.2, 1.39, 1.63, 1.98, 2.28, 2.98, 3.19, and 3.75 ppm.

2.5.2 Absolute Quantification

Following expert consensus recommendations [34], quantification of metabolite signal intensity to absolute concentrations was performed using the equation (Eq. 1; Supplementary Material S1) provided by Dhamala et al. [35]. T_1 and T_2 relaxation time constants of water at 7T were obtained from the literature [36,37]: T_1 (WM) = 1120 ms; T_2 (WM) = 55 ms; T_1 (GM)

= 2130 ms; T_2 (GM) = 50 ms; T_1 (CSF) = 4425 ms; T_2 (CSF) = 141 ms. Assumed visible water concentration was 36100 mmol/L in WM, 43300 mmol/L in GM, and 53800 mmol/L in CSF [35]. Voxel-specific tissue water concentrations were calculated per participant using Eq. 2 (Supplementary Material S1). Given that our TR >> TE, the T_2 relaxation times of metabolites, but not T_1, were included from the literature [38] (see Supplementary Table S2). Finally, GM, WM, and CSF volume fractions within the two MRS voxels were determined from structural data, and ranges are provided in Supplementary Table S3.

2.5.3 Quality Control

Data quality control was performed via visual inspection of the spectrum, fit, baseline, and residual, as per recommendation [39]. Signal-to-Noise Ratio (SNR) and Full-Width at Half Maximum (FWHM) were also inspected for each spectrum. Metabolites where the Cramér-Rao Lower Bound (CRLB) estimates (as provided by LCModel), averaged across all participants, exceeded 20% were considered unreliable and systematically excluded, following a commonly used threshold [6]. The resulting mean CRLBs for included metabolites per region of interest are shown in Supplementary Table S4.

2.6 Statistical Analysis

All statistical analyses were conducted in R (v4.4.1; R Core Team) within RStudio (v2024.09.0; RStudio, PBC, USA). General linear models (GLMs) were used to assess the relationship between metabolite levels and (a) age and (b) age groups, controlling for sex. To assess the effect of sex on age-related metabolite changes, participants were divided into two groups (i.e., men and women), and the associations with age and age group were performed independently within each sex. To investigate whether menopausal status impacts age-related metabolite level variations, women were categorized based on self-reported pre- and post-

menopausal status, with an age cut-off of 50 years of age (i.e., women < 50 years of age: pre-menopausal; women > 50 years of age: post-menopausal). Furthermore, to control for the peri-menopausal transition phase and self-reported variability, our final menopausal status groups were based on ± 5 years of the age cut-off, resulting in pre-menopausal women younger than 45 years of age, and post-menopausal women aged 55+ years of age. These ages were consistent with previously reported menopausal age ranges [40,41]. Additionally, to control for the effect of age in menopausal associations, the same analysis was performed in age-matched men (< 45 vs. > 55 years of age). Finally, GLMs, controlling for age, were performed to assess the effect of metabolite levels on functional test scores, in all participants, and in men and women separately. All statistical analyses were corrected for multiple comparisons using the false discovery rate (FDR) method at 5%. Statistical significance threshold was set at $p < 0.05$. Metabolite concentrations are reported in institutional units.

3. RESULTS

Participant demographics are provided in Table 1. Age groups were divided as follows: young adults: 20-39 years of age; middle-aged adults: 40-59 years of age; and old adults: 60-79 years of age. After performing quality control, five participants were excluded for analyses for PCC (four men and one woman in the older group) and one for CSWM (man in the younger group), resulting in 90 participants for PCC and 94 for CSWM. For all participants, there was 100% concordance between sex (biological) and gender (social), therefore the term "sex" is being used to describe both biological and social variables. All results are summarized in Table 2.

3.1 Age-Specific Metabolite Level Changes

3.1.1 Age as a Continuum

After controlling for sex, increasing age (20-79 years; Fig. 2) was associated with higher mI levels and lower Glu levels and in both PCC (mI: $p = 0.005$; Glu: $p = 0.003$) and CSWM (mI: $p = 0.005$; Glu: $p = 0.003$). In PCC, we found lower GSH levels ($p = 0.003$) with increasing age. Furthermore, in CSWM, increasing age was associated with (b) higher tCr ($p = 0.009$), (b) lower NAA ($p = 0.003$), and (c) higher NAAG ($p = 0.008$) levels.

3.1.2 Age Groups

When investigating metabolite level changes by age group (i.e., Middle-aged vs. Younger, Older vs. Younger, and Older vs. Middle-aged), we found similar results (Fig. 3). Specifically, in both PCC and CSWM, we found (a) higher mI levels (PCC: $p = 0.044$; CSWM: $p = 0.032$) in older adults relative to younger adults, and (b) lower Glu levels in middle-aged (PCC: $p = 0.049$; CSWM: $p = 0.010$) and older (PCC: $p = 0.001$; CSWM: $p = 0.003$) adults relative to

younger adults. In addition, in PCC, we found lower GSH levels in middle-aged (p = 0.036) and older (p = 0.003) adults compared to younger adults. In CSWM, relative younger adults, (a) middle-aged adults had higher levels of mI (p = 0.036) and lower levels of NAA (p = 0.026), and (b) older adults had higher tCr (p = 0.042), lower NAA (p = 0.001), and higher NAAG (p = 0.029) levels.

3.2 Sex-Specific Metabolite Level Changes

When investigating men and women as two independent groups (Fig. 4), we found that findings were driven by age-related changes in women.

3.2.1 Age as a Continuum

With increasing age, men did not demonstrate any significant metabolite level changes. In contrast, in women, increasing age was associated with lower Glu levels in both PCC (p = 0.022) and CSWM (p = 0.020). In PCC, women demonstrated lower GSH levels (p = 0.022) with increasing age. Finally, in CSWM, increasing age in women was associated with (a) higher levels of mI (p = 0.018), tCr (p = 0.018), tCho (p = 0.018), and NAAG (p = 0.040), and (b) lower NAA levels (p = 0.024).

3.2.2 Age Groups

Within-sex analyses showed no significant differences in metabolite levels across age groups in men. In women, age group effects were pronounced. Older women had significantly lower Glu levels in PCC (p = 0.019) and CSWM (p = 0.024) than younger women. In addition, in PCC, GSH levels were lower in older relative to younger women (p = 0.024). In CSWM, (a) middle-aged women had higher mI (p = 0.011) levels relative to younger women, and (b) older women had higher levels of mI (p = 0.024) and tCr (p = 0.024), and lower NAA levels (p =

0.024) compared to younger women. Finally, higher tCho levels in older women compared to younger women were borderline significant in CSWM (p = 0.054).

3.2.3 Menopausal Status

To investigate whether metabolite level changes differed by menopausal status, women were stratified based on their self-reported status (± 5 years to control for those undergoing a peri-menopausal transition phase). In particular, 19 women were pre-menopaused (30.53 ± 7.19 years of age) and 21 were post-menopaused (66.71 ± 7.31 years of age). In particular, we found that, relative to pre-menopausal women, post-menopausal women had (a) lower Glu levels in PCC ($p_{unadjusted}$ = 0.022) and CSWM ($p_{unadjusted}$ = 0.015), (b) higher tCho levels in PCC ($p_{unadjusted}$ = 0.044) and CSWM ($p_{unadjusted}$ = 0.006), (c) lower GSH levels ($p_{unadjusted}$ = 0.024) in PCC, and (c) higher levels of mI ($p_{unadjusted}$ = 0.014) and tCr ($p_{unadjusted}$ = 0.004) in CSWM, but none of these results survived multiple comparisons correction. Notably, with multiple comparisons correction, differences in tCho and tCr levels in CSWM between pre- and post-menopausal women were borderline significant (p = 0.058).

When comparing men older than 55 years (N = 19; 67.00 ± 7.37 years of age) relative to those younger than 45 years (N = 18; 31.33 ± 6.02 years of age), we found that older men had (a) lower Glu levels in PCC ($p_{unadjusted}$ = 0.013) and CSWM ($p_{unadjusted}$ = 0.045), (b) lower GSH levels ($p_{unadjusted}$ = 0.043) and higher mI levels ($p_{unadjusted}$ = 0.011) levels in PCC, and (c) lower NAA levels ($p_{unadjusted}$ = 0.010) in CSWM, but none of these results survived multiple comparisons correction.

3.3 Metabolite Levels and Functional Test Scores

No association between metabolite levels and functional test scores remained significant after correcting for multiple comparisons correction. Without correction, we found a positive association between 9HPT score and tCho levels in PCC ($p_{unadjusted}$ = 0.033). In women, 9HPT score was negatively associated with mI ($p_{unadjusted}$ = 0.048) and NAAG ($p_{unadjusted}$ = 0.006) levels in CSWM. Finally, in men, we found positive associations between (a) SDMT score and NAA levels in CSWM ($p_{unadjusted}$ = 0.047), and (b) 9HPT score and Gln levels in CSWM ($p_{unadjusted}$ = 0.037).

With increasing age, there was a negative association with the SDMT score ($p < 0.001$), and positive associations with the T25FW ($p = 0.029$) and 9HPT ($p < 0.001$) scores. Specifically, middle-aged ($p < 0.001$) and older adults ($p < 0.001$) had lower SDMT scores (i.e., worse processing speed) than younger adults, and older adults ($p < 0.001$) also had lower scores compared to middle-aged adults. In addition, (a) older adults had a higher T25FW score (i.e., longer time to walk 25 feet) than younger adults ($p = 0.015$), (b) older adults had a higher 9HPT score (i.e., worse manual dexterity) relative to both middle-aged ($p = 0.017$) and younger ($p < 0.001$) adults, and (c) middle-aged adults had a higher 9HPT score compared to younger adults ($p = 0.044$). Sex-specific analyses revealed that age was (a) negatively associated with the SMDT score (women: $p < 0.001$; men: $p < 0.001$) and (b) positively associated with the 9HPT score (women: $p = 0.002$; men: $p = 0.001$).

4. DISCUSSION

Our study examines the healthy adult lifespan, from younger to older age, with particular focus on midlife, a period often underrepresented in research but critical for future health [2,3]. Using state-of-the-art UHF MRS with expert consensus methods [34,39], we precisely quantified eight metabolites, including three low-concentration metabolites, revealing age-related metabolic changes in the brain. These metabolic pathways in different brain cell types have been summarized in Figure 5. Our results indicate that early signatures of OS, neuroinflammation, and neuronal vulnerability emerge in midlife, reflected by changes in (a) GSH, (b) mI, tCr, and tCho, and (c) NAA, NAAG, and Glu levels, respectively. These interconnected processes appear fundamental to brain aging, and may contribute to onset and progression of NDDs such as AD [7,42,43]. Importantly, they align with current therapeutic priorities, as evidenced by the 2025 AD drug development pipeline, which includes 31% of agents targeting metabolism, OS, neuroinflammation, and neuronal processes [44].

4.1 Age-Related Metabolite Changes in Healthy Aging

4.1.1 Midlife Antioxidant Decline in Healthy Aging

In our cross-sectional UHF MRS study, levels of the antioxidant GSH in the PCC showed a negative association with age as a continuous measure, and age-group comparisons demonstrated reduced concentrations by midlife, highlighting early vulnerability to OS. Parallel to our findings, a prior 7T MRS study reported a negative association between GSH levels and age in the anterior cingulate cortex in healthy adults (20-54 years), although midlife-specific changes were not assessed [45]. Although MRS studies measuring GSH remain limited due to its complex structure complicating quantification at lower field

strengths [7], these observations suggest that OS in GM may increase earlier in adulthood than previously recognized.

This vulnerability is reinforced by the high metabolic demand of GM, which consumes over twice the oxygen of WM and contains more mitochondria to support adenosine triphosphate (ATP) production via oxidative phosphorylation – the predominant ROS source [5,46]. Elevated energetic burden renders GM, and particularly highly-connected hub regions like the PCC [11,12,23], prone to OS, which is further amplified by the midlife GSH decline observed in our study. While modest OS is typical with aging, excessive elevations may signal early neuropathological risk [5], consistent with evidence of reduced antioxidant capacity in PCC in AD [47]. Measuring GSH in PCC using UHF MRS could therefore provide an early marker of abnormal metabolic shifts and a targetable window for intervention [7,48].

4.1.2 Midlife Neuroinflammation in Healthy Aging

Importantly, OS in midlife may act in concert with neuroinflammatory processes, further contributing to early brain vulnerability. In our study, age-group comparisons revealed elevated mI levels in midlife in CSWM, while continuous age analyses showed generally higher mI with increasing age in both PCC and CSWM. Only one prior 7T MRS study included middle-aged adults and reported higher mI levels without directly assessing WM [49], highlighting the novelty of our reported higher WM mI in midlife. Our findings likely reflect early WM neuroinflammation, as mI is predominantly localized in glial cells and its elevation has been linked to astrogliosis [13] and systemic inflammation [49,50], supporting its interpretation as an *in vivo* marker of neuroimmune activity. This interpretation is further reinforced by complementary evidence from postmortem immunohistochemistry of brain

tissue and *in vivo* PET imaging using [^{11}C]-(R)-PK11195 – a ligand targeting activated microglia – both demonstrating increased WM neuroimmune activation beginning in midlife [51]. In NDDs, including AD, WM neuroinflammation has been reported to precede symptom onset [52], and increased MRS-detected mI levels have been found early in the AD continuum [53], highlighting its potential role as a biomarker of neurodegenerative processes.

Similar to mI, tCr is higher in glial cells than neurons, and has been associated with neuroinflammation [49,54]. We observed age-related increases in tCr in CSWM, with significant differences between older and younger adults. This pattern aligns with most MRS studies reporting tCr elevations with age in both PCC and CSWM [15,16,55,56]. Since creatine exhibits antioxidant and anti-inflammatory properties [57], these increases in healthy aging may reflect a compensatory mechanism to altered energy demands [56]. By contrast, reduced tCr levels in AD [58] could indicate a breakdown of this compensatory mechanism, along with overall reduced metabolic activity due to neurodegeneration.

Together, these findings suggest that both mI and tCr serve as sensitive biomarkers of early neuroinflammatory changes, potentially heralding vulnerability to neurodegeneration in AD.

4.1.3 Midlife Neuronal Vulnerability in Healthy Aging

OS and neuroinflammation can both contribute to neurodegeneration and NDDs [42]. In CSWM, we observed lower NAA levels with increasing age, with age-group comparisons showing decreases starting in middle-aged adults. Given that NAA is an established neuroaxonal integrity marker [13], our results point to emerging neuroaxonal impairment beginning in midlife. This interpretation is supported by a study combining MRS and diffusion tensor imaging in middle-aged-to-older adults demonstrating WM ultrastructure

alterations [59], although younger adults and age-group differences were not examined. In most NDDs, including AD, decreased NAA levels have been reported, reflective of neuronal dysfunction and/or loss and mitochondrial dysfunction [58,60].

In contrast to NAA, literature on the neuromodulator NAAG is sparse, given its much lower concentration and quantification complexity (especially at lower field strengths), which often leads to its combination with NAA as total NAA [15,16]. We found higher levels of NAAG in CSWM with increasing age. Only one 7T study assessed NAAG levels and found decreases in older relative to younger adults [22], without investigating WM or middle-aged adults, highlighting the novelty of our finding. High NAAG levels are considered neuroprotective and have been found to have a positive effect on cognition [61]. It also modulates Glu release, therefore preventing Glu-induced excitotoxicity [61]. Given its action on Glu receptors and decreased levels reported in several NDDs, including AD, NAAG has become a focus of clinical trials [61,62].

In fact, our study provides novel evidence that Glu levels decrease in the PCC and CSWM starting in midlife. Prior 7T MRS studies observed lower Glu only in GM and at older ages, leaving midlife unexplored [22,49]. In PCC, lower midlife Glu levels likely reflect disruptions in the neuronal-astrocytic Glu-Gln cycle, involving several proteins, transporters, and receptors, leading to impaired Glu homeostasis and vulnerability to neurotoxicity [63,64]. In contrast, in CSWM, lower Glu levels may reflect compromised neuroaxonal integrity and neuroinflammation, which is supported by our findings of lower NAA levels and higher mI and tCr levels, respectively. While these changes reflect normal aging, Glu levels decline further in AD, indicating progressive metabolic and neuronal compromise linked to memory impairment [65].

Overall, these findings suggest that NAA and Glu may serve as biomarkers of increased neuronal vulnerability, while NAAG may be linked to neuroprotection in healthy aging and possibly provide a therapeutic target in AD.

4.2 Sex-Related Metabolite Changes in Healthy Aging

Our sex-specific analyses revealed that the observed metabolite changes were driven primarily by women, with no significant effects in men. In women, increasing age was associated with lower GSH levels in PCC, indicating reduced antioxidant capacity, and lower Glu levels, reflecting increased neuronal vulnerability. In CSWM, increasing age corresponded to higher levels of mI, tCr, and tCho, indicative of elevated neuroinflammation, alongside lower Glu and NAA levels, suggesting greater WM compromise.

These age-related sex-specific differences in metabolite levels might be due to estrogen and other estrogenic compounds. In particular, estrogen possesses antioxidant and anti-inflammatory properties, by protecting mitochondrial function [66] and lowering pro-inflammatory markers [67], respectively. Estrogen also protects neuronal integrity by reducing Glu-induced excitotoxicity [68] and increasing NMDA availability [69]. However, this estrogen-related advantage is lost after menopause [70], typically occurring between 45-55 years of age [40,41]. Therefore, post-menopausal estrogen loss might accelerate OS, enhance neuroinflammation, and alter neuronal systems [71], overall contributing to the greater AD risk in women [72].

4.3 Limitations

Our study has potential limitations. First, while using state-of-the-art scanning techniques, we used two single-voxels only, due to the long MRS acquisition duration and participants'

ability/willingness to remain still in the scanner. We used a single-voxel technique rather than spectroscopic imaging in order to have sufficient spectral quality to reliably measure metabolites with low concentrations and J-coupled resonances, such as GSH. Secondly, for absolute quantification of metabolite signal intensity, similar to other studies [34,35], relaxation times were acquired from the literature rather than measured, due to scan time limitations. Moreover, while age-related decreases of T_2 relaxation times for NAA, tCr, and tCho have been reported [73], we used one T_2 value per metabolite for all participants to minimize bias, as very few studies reported T_2 acquired at 7T [36–38] and none covered all three age groups (especially middle-aged). Finally, we did not have biological tests available to assess hormonal levels, only self-reported menopausal status, emphasizing the need for sex-specific studies with standardized staging (e.g., Stages of Reproductive Aging Workshop guidelines [74]).

5. CONCLUSION

In conclusion, our cross-sectional study using state-of-the-art UHF MRS offers new insights into normative metabolite data across the healthy adult lifespan, including midlife and sex-specific patterns. In particular, we reported that OS, neuroinflammation, and neuronal vulnerability emerge as early as healthy midlife, highlighting a potentially pivotal window for brain health. In addition, our study provides evidence of sex-specific metabolic aging, with a potential sex hormone-related advantage of women (e.g., estrogen) lost after menopause, therefore contributing to greater OS, neuroinflammation, and neuronal vulnerability. Future studies should focus more on middle-aged healthy adults and the transition from pre- to post-menopause in middle-aged women, to better understand the mechanisms underlying sex-specific brain aging.

6. REFERENCES

[1] Sun X, Li X. Editorial: Aging and chronic disease: public health challenge and education reform. Front Public Health 2023;11:1175898. https://doi.org/10.3389/fpubh.2023.1175898.

[2] Dohm-Hansen S, English JA, Lavelle A, Fitzsimons CP, Lucassen PJ, Nolan YM. The "middle-aging" brain. Trends Neurosci 2024;47:259–72. https://doi.org/10.1016/j.tins.2024.02.001.

[3] Ritchie K, Ritchie CW, Yaffe K, Skoog I, Scarmeas N. Is late-onset Alzheimer's disease really a disease of midlife? Alzheimers Dement (N Y) 2015;1:122–30. https://doi.org/10.1016/j.trci.2015.06.004.

[4] Livingston G, Huntley J, Liu KY, Costafreda SG, Selbæk G, Alladi S, et al. Dementia prevention, intervention, and care: 2024 report of the Lancet standing Commission. Lancet 2024;404:572–628. https://doi.org/10.1016/S0140-6736(24)01296-0.

[5] Iakovou E, Kourti M. A Comprehensive Overview of the Complex Role of Oxidative Stress in Aging, The Contributing Environmental Stressors and Emerging Antioxidant Therapeutic Interventions. Front Aging Neurosci 2022;14:827900. https://doi.org/10.3389/fnagi.2022.827900.

[6] Bottino F, Lucignani M, Napolitano A, Dellepiane F, Visconti E, Rossi Espagnet MC, et al. In Vivo Brain GSH: MRS Methods and Clinical Applications. Antioxidants (Basel) 2021;10. https://doi.org/10.3390/antiox10091407.

[7] Detcheverry F, Senthil S, Narayanan S, Badhwar A. Changes in levels of the antioxidant glutathione in brain and blood across the age span of healthy adults: A systematic review. Neuroimage Clin 2023;40:103503. https://doi.org/10.1016/j.nicl.2023.103503.

[8] Lushchak VI. Interplay between bioenergetics and oxidative stress at normal brain aging. Aging as a result of increasing disbalance in the system oxidative stress-energy

provision. Pflugers Arch 2021;473:713–22. https://doi.org/10.1007/s00424-021-02531-4.

[9] Doshi SB, Agarwal A. The role of oxidative stress in menopause. J Midlife Health 2013;4:140–6. https://doi.org/10.4103/0976-7800.118990.

[10] Grimm A, Eckert A. Brain aging and neurodegeneration: from a mitochondrial point of view. J Neurochem 2017;143:418–31. https://doi.org/10.1111/jnc.14037.

[11] Leech R, Sharp DJ. The role of the posterior cingulate cortex in cognition and disease. Brain 2014;137:12–32. https://doi.org/10.1093/brain/awt162.

[12] Rahim F, Khalafi M, Davoodi M, Shirbandi K. Metabolite changes in the posterior cingulate cortex could be a signature for early detection of Alzheimer's disease: a systematic review and meta-analysis study based on 1H-NMR. Egypt J Neurol Psychiatr Neurosurg 2023;59. https://doi.org/10.1186/s41983-023-00649-z.

[13] Duarte JMN, Lei H, Mlynárik V, Gruetter R. The neurochemical profile quantified by in vivo 1H NMR spectroscopy. Neuroimage 2012;61:342–62. https://doi.org/10.1016/j.neuroimage.2011.12.038.

[14] Haga KK, Khor YP, Farrall A, Wardlaw JM. A systematic review of brain metabolite changes, measured with 1H magnetic resonance spectroscopy, in healthy aging. Neurobiol Aging 2009;30:353–63. https://doi.org/10.1016/j.neurobiolaging.2007.07.005.

[15] Cleeland C, Pipingas A, Scholey A, White D. Neurochemical changes in the aging brain: A systematic review. Neurosci Biobehav Rev 2019;98:306–19. https://doi.org/10.1016/j.neubiorev.2019.01.003.

[16] Cichocka M, Bereś A. From fetus to older age: A review of brain metabolic changes across the lifespan. Ageing Res Rev 2018;46:60–73. https://doi.org/10.1016/j.arr.2018.05.005.

[17] Villemagne VL, Burnham S, Bourgeat P, Brown B, Ellis KA, Salvado O, et al. Amyloid β deposition, neurodegeneration, and cognitive decline in sporadic Alzheimer's

disease: a prospective cohort study. Lancet Neurol 2013;12:357–67. https://doi.org/10.1016/S1474-4422(13)70044-9.

[18] Jack CR Jr, Knopman DS, Jagust WJ, Petersen RC, Weiner MW, Aisen PS, et al. Tracking pathophysiological processes in Alzheimer's disease: an updated hypothetical model of dynamic biomarkers. Lancet Neurol 2013;12:207–16. https://doi.org/10.1016/S1474-4422(12)70291-0.

[19] McIntyre DJO, Charlton RA, Markus HS, Howe FA. Long and short echo time proton magnetic resonance spectroscopic imaging of the healthy aging brain. J Magn Reson Imaging 2007;26:1596–606. https://doi.org/10.1002/jmri.21198.

[20] Pradhan S, Bonekamp S, Gillen JS, Rowland LM, Wijtenburg SA, Edden RAE, et al. Comparison of single voxel brain MRS AT 3T and 7T using 32-channel head coils. Magn Reson Imaging 2015;33:1013–8. https://doi.org/10.1016/j.mri.2015.06.003.

[21] Terpstra M, Cheong I, Lyu T, Deelchand DK, Emir UE, Bednařík P, et al. Test-retest reproducibility of neurochemical profiles with short-echo, single-voxel MR spectroscopy at 3T and 7T. Magn Reson Med 2016;76:1083–91. https://doi.org/10.1002/mrm.26022.

[22] Marjańska M, McCarten JR, Hodges J, Hemmy LS, Grant A, Deelchand DK, et al. Region-specific aging of the human brain as evidenced by neurochemical profiles measured noninvasively in the posterior cingulate cortex and the occipital lobe using 1H magnetic resonance spectroscopy at 7 T. Neuroscience 2017;354:168–77. https://doi.org/10.1016/j.neuroscience.2017.04.035.

[23] Badhwar A, Tam A, Dansereau C, Orban P, Hoffstaedter F, Bellec P. Resting-state network dysfunction in Alzheimer's disease: A systematic review and meta-analysis. Alzheimers Dement 2017;8:73–85. https://doi.org/10.1016/j.dadm.2017.03.007.

[24] Kim HJ, Cho H, Park M, Kim JW, Ahn SJ, Lyoo CH, et al. MRI-visible perivascular spaces in the centrum semiovale are associated with brain amyloid deposition in patients with

Alzheimer disease-related cognitive impairment. AJNR Am J Neuroradiol 2021;42:1231–8. https://doi.org/10.3174/ajnr.A7155.

[25] Sporn L, MacMillan EL, Ge R, Greenway K, Vila-Rodriguez F, Laule C. Longer repetition time proton MR spectroscopy shows increasing hippocampal and parahippocampal metabolite concentrations with aging. J Neuroimaging 2019;29:592–7. https://doi.org/10.1111/jon.12648.

[26] Rao SM, Losinski G, Mourany L, Schindler D, Mamone B, Reece C, et al. Processing speed test: Validation of a self-administered, iPad((R))-based tool for screening cognitive dysfunction in a clinic setting. Mult Scler 2017;23:1929–37.

[27] Marques JP, Kober T, Krueger G, van der Zwaag W, Van de Moortele P-F, Gruetter R. MP2RAGE, a self bias-field corrected sequence for improved segmentation and T1-mapping at high field. Neuroimage 2010;49:1271–81. https://doi.org/10.1016/j.neuroimage.2009.10.002.

[28] Glick Y, Garg V. Centrum semiovale. Radiopaedia.org 2014. https://doi.org/10.53347/rid-30579.

[29] Gruetter R. Automatic, localized in vivo adjustment of all first- and second-order shim coils. Magn Reson Med 1993;29:804–11. https://doi.org/10.1002/mrm.1910290613.

[30] Tkáč I, Deelchand D, Dreher W, Hetherington H, Kreis R, Kumaragamage C, et al. Water and lipid suppression techniques for advanced 1 H MRS and MRSI of the human brain: Experts' consensus recommendations. NMR Biomed 2021;34:e4459. https://doi.org/10.1002/nbm.4459.

[31] Isensee F, Jaeger PF, Kohl SAA, Petersen J, Maier-Hein KH. nnU-Net: a self-configuring method for deep learning-based biomedical image segmentation. Nat Methods 2021;18:203–11. https://doi.org/10.1038/s41592-020-01008-z.

[32] Simpson R, Devenyi GA, Jezzard P, Hennessy TJ, Near J. Advanced processing and

simulation of MRS data using the FID appliance (FID-A)-An open source, MATLAB-based toolkit. Magn Reson Med 2017;77:23–33. https://doi.org/10.1002/mrm.26091.

[33] Provencher SW. Automatic quantitation of localized in vivo 1H spectra with LCModel. NMR Biomed 2001;14:260–4. https://doi.org/10.1002/nbm.698.

[34] Near J, Harris AD, Juchem C, Kreis R, Marjańska M, Öz G, et al. Preprocessing, analysis and quantification in single-voxel magnetic resonance spectroscopy: experts' consensus recommendations. NMR Biomed 2021;34:e4257. https://doi.org/10.1002/nbm.4257.

[35] Dhamala E, Abdelkefi I, Nguyen M, Hennessy TJ, Nadeau H, Near J. Validation of in vivo MRS measures of metabolite concentrations in the human brain. NMR Biomed 2019;32:e4058. https://doi.org/10.1002/nbm.4058.

[36] Rooney WD, Johnson G, Li X, Cohen ER, Kim S-G, Ugurbil K, et al. Magnetic field and tissue dependencies of human brain longitudinal 1H2O relaxation in vivo. Magn Reson Med 2007;57:308–18. https://doi.org/10.1002/mrm.21122.

[37] Bartha R, Michaeli S, Merkle H, Adriany G, Andersen P, Chen W, et al. In vivo 1H2O T2+ measurement in the human occipital lobe at 4T and 7T by Carr-Purcell MRI: detection of microscopic susceptibility contrast. Magn Reson Med 2002;47:742–50. https://doi.org/10.1002/mrm.10112.

[38] Swanberg KM, Prinsen H, Coman D, de Graaf RA, Juchem C. Quantification of glutathione transverse relaxation time T2 using echo time extension with variable refocusing selectivity and symmetry in the human brain at 7 Tesla. J Magn Reson 2018;290:1–11. https://doi.org/10.1016/j.jmr.2018.02.017.

[39] Wilson M, Andronesi O, Barker PB, Bartha R, Bizzi A, Bolan PJ, et al. Methodological consensus on clinical proton MRS of the brain: Review and recommendations. Magn Reson Med 2019;82:527–50. https://doi.org/10.1002/mrm.27742.

[40] Davis SR, Baber RJ. Treating menopause - MHT and beyond. Nat Rev Endocrinol 2022;18:490–502. https://doi.org/10.1038/s41574-022-00685-4.

[41] Peacock K, Carlson K, Ketvertis KM. Menopause. StatPearls, Treasure Island (FL): StatPearls Publishing; 2025.

[42] Dash UC, Bhol NK, Swain SK, Samal RR, Nayak PK, Raina V, et al. Oxidative stress and inflammation in the pathogenesis of neurological disorders: Mechanisms and implications. Acta Pharm Sin B 2025;15:15–34. https://doi.org/10.1016/j.apsb.2024.10.004.

[43] Detcheverry FE, Senthil S, Motue WLK, Hosein C, Arnaoutelis R, Araujo D, et al. Investigating the oxidative stress–vascular brain injury axis in mild cognitive impairment of the Alzheimer's type. Alzheimers Dement 2025. https://doi.org/10.1002/alz.70456.

[44] Cummings JL, Zhou Y, Lee G, Zhong K, Fonseca J, Leisgang-Osse AM, et al. Alzheimer's disease drug development pipeline: 2025. Alzheimers Dement (N Y) 2025;11:e70098. https://doi.org/10.1002/trc2.70098.

[45] Lally N, An L, Banerjee D, Niciu MJ, Luckenbaugh DA, Richards EM, et al. Reliability of 7T ^{1}H-MRS measured human prefrontal cortex glutamate, glutamine, and glutathione signals using an adapted echo time optimized PRESS sequence: A between- and within-sessions investigation. Journal of Magnetic Resonance Imaging 2016;43:88–98. https://doi.org/10.1002/jmri.24970.

[46] Zhu X-H, Qiao H, Du F, Xiong Q, Liu X, Zhang X, et al. Quantitative imaging of energy expenditure in human brain. Neuroimage 2012;60:2107–17. https://doi.org/10.1016/j.neuroimage.2012.02.013.

[47] Shukla D, Mandal PK, Tripathi M, Vishwakarma G, Mishra R, Sandal K. Quantitation of in vivo brain glutathione conformers in cingulate cortex among age-matched control, MCI, and AD patients using MEGA-PRESS. Hum Brain Mapp 2020;41:194–217. https://doi.org/10.1002/hbm.24799.

[48] Glutathione for Alzheimer's Disease n.d. https://www.alzheimers.gov/clinical-trials/glutathione-alzheimers-disease (accessed November 3, 2025).

[49] Lind A, Boraxbekk C-J, Petersen ET, Paulson OB, Siebner HR, Marsman A. Regional myo-inositol, creatine, and choline levels are higher at older age and scale negatively with visuospatial working memory: A cross-sectional proton MR spectroscopy study at 7 Tesla on normal cognitive ageing. J Neurosci 2020;40:8149–59. https://doi.org/10.1523/JNEUROSCI.2883-19.2020.

[50] Lind A, Boraxbekk C-J, Petersen ET, Paulson OB, Andersen O, Siebner HR, et al. Do glia provide the link between low-grade systemic inflammation and normal cognitive ageing? A 1 H magnetic resonance spectroscopy study at 7 tesla. J Neurochem 2021;159:185–96. https://doi.org/10.1111/jnc.15456.

[51] Raj D, Yin Z, Breur M, Doorduin J, Holtman IR, Olah M, et al. Increased white matter inflammation in aging- and Alzheimer's disease brain. Front Mol Neurosci 2017;10:206. https://doi.org/10.3389/fnmol.2017.00206.

[52] Wang Q, Schindler SE, Chen G, Mckay NS, McCullough A, Flores S, et al. Investigating white matter neuroinflammation in Alzheimer disease using diffusion-based neuroinflammation imaging. Neurology 2024;102:e208013. https://doi.org/10.1212/WNL.0000000000208013.

[53] Chaudhary S, Chao HH, Agarwal K, Gupta S, Li C-SR. Imaging markers of neuroinflammation in aging and Alzheimer's disease and related dementia: A comprehensive review. Neurosci Biobehav Rev 2025;176:106270. https://doi.org/10.1016/j.neubiorev.2025.106270.

[54] Urenjak J, Williams SR, Gadian DG, Noble M. Proton nuclear magnetic resonance spectroscopy unambiguously identifies different neural cell types. J Neurosci 1993;13:981–9. https://doi.org/10.1523/jneurosci.13-03-00981.1993.

[55] Gong T, Hui SCN, Zöllner HJ, Britton M, Song Y, Chen Y, et al. Neurometabolic timecourse of healthy aging 2022. https://doi.org/10.1101/2022.06.08.495050.

[56] Mahmoudi N, Dadak M, Bronzlik P, Maudsley AA, Sheriff S, Lanfermann H, et al. Microstructural and metabolic changes in normal aging human brain studied with combined whole-brain MR spectroscopic imaging and quantitative MR imaging. Clin Neuroradiol 2023;33:993–1005. https://doi.org/10.1007/s00062-023-01300-3.

[57] Deminice R, Rosa FT, Franco GS, Jordao AA, de Freitas EC. Effects of creatine supplementation on oxidative stress and inflammatory markers after repeated-sprint exercise in humans. Nutrition 2013;29:1127–32. https://doi.org/10.1016/j.nut.2013.03.003.

[58] Song T, Song X, Zhu C, Patrick R, Skurla M, Santangelo I, et al. Mitochondrial dysfunction, oxidative stress, neuroinflammation, and metabolic alterations in the progression of Alzheimer's disease: A meta-analysis of in vivo magnetic resonance spectroscopy studies. Ageing Res Rev 2021;72:101503. https://doi.org/10.1016/j.arr.2021.101503.

[59] Charlton RA, Barrick TR, McIntyre DJ, Shen Y, O'Sullivan M, Howe FA, et al. White matter damage on diffusion tensor imaging correlates with age-related cognitive decline. Neurology 2006;66:217–22. https://doi.org/10.1212/01.wnl.0000194256.15247.83.

[60] McKiernan E, Su L, O'Brien J. MRS in neurodegenerative dementias, prodromal syndromes and at-risk states: A systematic review of the literature. NMR Biomed 2023;36:e4896. https://doi.org/10.1002/nbm.4896.

[61] Morland C, Nordengen K. N-acetyl-aspartyl-glutamate in brain health and disease. Int J Mol Sci 2022;23:1268. https://doi.org/10.3390/ijms23031268.

[62] Bukke VN, Archana M, Villani R, Romano AD, Wawrzyniak A, Balawender K, et al. The dual role of glutamatergic neurotransmission in Alzheimer's disease: From pathophysiology to pharmacotherapy. Int J Mol Sci 2020;21:7452. https://doi.org/10.3390/ijms21207452.

[63] Matias I, Diniz LP, Araujo APB, Damico IV, de Moura P, Cabral-Miranda F, et al. Age-associated upregulation of glutamate transporters and glutamine synthetase in senescent astrocytes in vitro and in the mouse and human hippocampus. ASN Neuro 2023;15:17590914231157974. https://doi.org/10.1177/17590914231157974.

[64] Gasiorowska A, Wydrych M, Drapich P, Zadrozny M, Steczkowska M, Niewiadomski W, et al. The biology and pathobiology of glutamatergic, cholinergic, and dopaminergic signaling in the aging brain. Front Aging Neurosci 2021;13:654931. https://doi.org/10.3389/fnagi.2021.654931.

[65] Wong D, Atiya S, Fogarty J, Montero-Odasso M, Pasternak SH, Brymer C, et al. Reduced hippocampal glutamate and posterior cingulate N-acetyl aspartate in mild cognitive impairment and Alzheimer's disease is associated with episodic memory performance and white matter integrity in the cingulum: A pilot study. J Alzheimers Dis 2020;73:1385–405. https://doi.org/10.3233/JAD-190773.

[66] Borrás C, Gambini J, López-Grueso R, Pallardó FV, Viña J. Direct antioxidant and protective effect of estradiol on isolated mitochondria. Biochim Biophys Acta 2010;1802:205–11. https://doi.org/10.1016/j.bbadis.2009.09.007.

[67] Karim R, Stanczyk FZ, Hodis HN, Cushman M, Lobo RA, Hwang J, et al. Associations between markers of inflammation and physiological and pharmacological levels of circulating sex hormones in postmenopausal women. Menopause 2010;17:785–90. https://doi.org/10.1097/gme.0b013e3181cc50b2.

[68] Goyette MJ, Murray SL, Saldanha CJ, Holton K. Sex hormones, neurosteroids, and glutamatergic neurotransmission: A review of the literature. Neuroendocrinology 2023;113:905–14. https://doi.org/10.1159/000531148.

[69] Bendis PC, Zimmerman S, Onisiforou A, Zanos P, Georgiou P. The impact of estradiol on serotonin, glutamate, and dopamine systems. Front Neurosci 2024;18:1348551.

https://doi.org/10.3389/fnins.2024.1348551.

[70] Martínez de Toda I, González-Sánchez M, Díaz-Del Cerro E, Valera G, Carracedo J, Guerra-Pérez N. Sex differences in markers of oxidation and inflammation. Implications for ageing. Mech Ageing Dev 2023;211:111797. https://doi.org/10.1016/j.mad.2023.111797.

[71] Henderson VW. Cognitive changes after menopause: influence of estrogen. Clin Obstet Gynecol 2008;51:618–26. https://doi.org/10.1097/GRF.0b013e318180ba10.

[72] Mervosh N, Devi G. Estrogen, menopause, and Alzheimer's disease: understanding the link to cognitive decline in women. Front Mol Biosci 2025;12:1634302. https://doi.org/10.3389/fmolb.2025.1634302.

[73] Marjańska M, Emir UE, Deelchand DK, Terpstra M. Faster metabolite (1)H transverse relaxation in the elder human brain. PLoS One 2013;8:e77572. https://doi.org/10.1371/journal.pone.0077572.

[74] Soules M, Sherman S, Parrott E, Rebar R, Santoro N, Utian W, et al. Executive summary: Stages of Reproductive Aging Workshop (STRAW). Climacteric 2001;4:267–72. https://doi.org/10.1080/cmt.4.4.267.272.

ACKNOWLEDGMENTS

The authors would like to thank Ali Filali-Mouhim, PhD, from the Centre de Recherche de l'Institut Universitaire de Gériatrie de Montréal (CRIUGM) for his input in the statistical analysis, and Lianne Trigiani, PhD, for reading and providing feedback on the manuscript. The authors would also like to thank all the participants in this study for their time.

CONFLICT OF INTEREST STATEMENT

All authors declare that they have no financial, personal, or competing interests/conflicts.

CONSENT STATEMENT

Ethical approval was obtained from the aging-neuroimaging research ethics committee of the *CIUSSS du Centre-Sud-de-île-de-Montréal* (CIUSSS-CSMTL), and from the McGill University Institutional Review Board, Faculty of Medicine and Health Sciences. Written informed consent was obtained from all participants.

FUNDING SOURCES

This work was supported by the Réseau de Bio-Imagerie du Québec (RBIQ) Pilot Grant, the Centre de Recherche de l'Institut Universitaire de Gériatrie de Montréal (CRIUGM) programme d'appui à des Projets de Recherche Stratégiques et Structurants (PRSS), and the

Fonds de Recherche Québec – Santé (FRQS) (A.B); the Canadian Institutes of Health Research grant (CIHR) (S.N., #153005); as well as FRQS Chercheurs boursiers Junior 1 and 2, and the Fonds de soutien à la recherche pour les neurosciences du vieillissement from the Fondation Courtois (A.B.); and the FRQS bourse de formation au doctorat (2024) (#352199, F.E.D.; #332672, S.S).

KEYWORDS

Oxidative stress; Glutathione; Healthy aging; Magnetic resonance spectroscopy; Middle-age; Sex-specific; Neuroinflammation; Neuronal vulnerability.

FIGURE LEGENDS

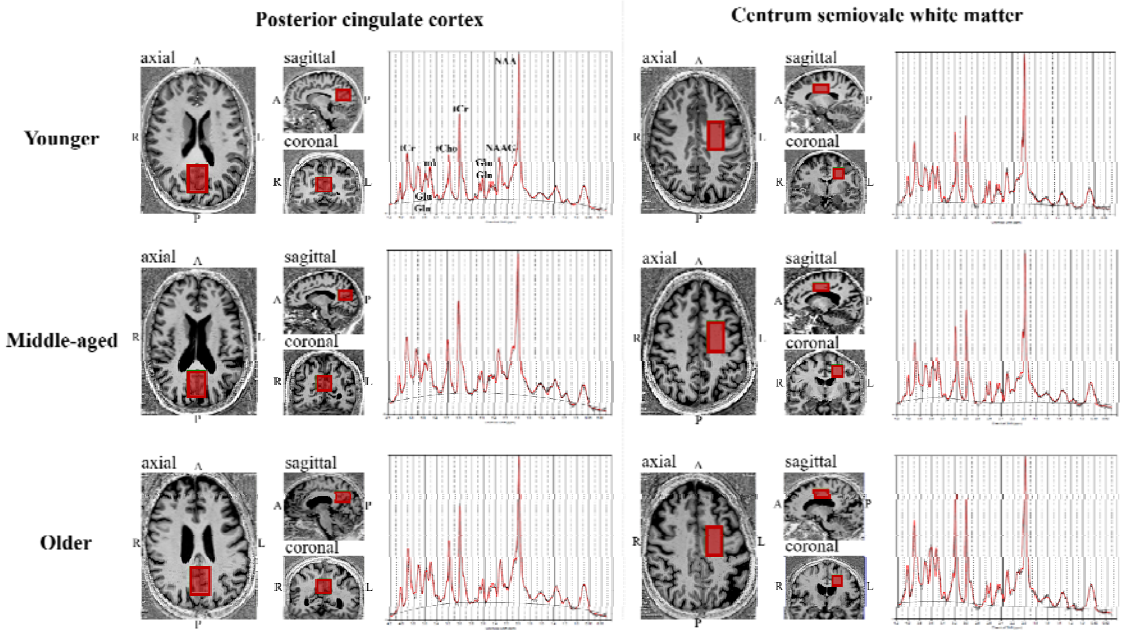

Figure 1. Single-voxel (red boxes) placement per age group (i.e., Younger, Middle-aged, Older) in posterior cingulate cortex/precuneus; and left centrum semiovale white matter. *Abbreviations:* Gln, glutamine; Glu, glutamate; mI, *myo*-inositol; NAA, *N*-acetylaspartate; NAAG, *N*-acetylaspartyl-glutamate; PCr, phosphocreatine; RL x AP x FH, right-left x anterior-posterior x foot-head; tCho, total choline; tCr, total creatine. Glutathione (GSH) was not labeled on the example spectrum due to its complex structure with multiple overlapping resonances.

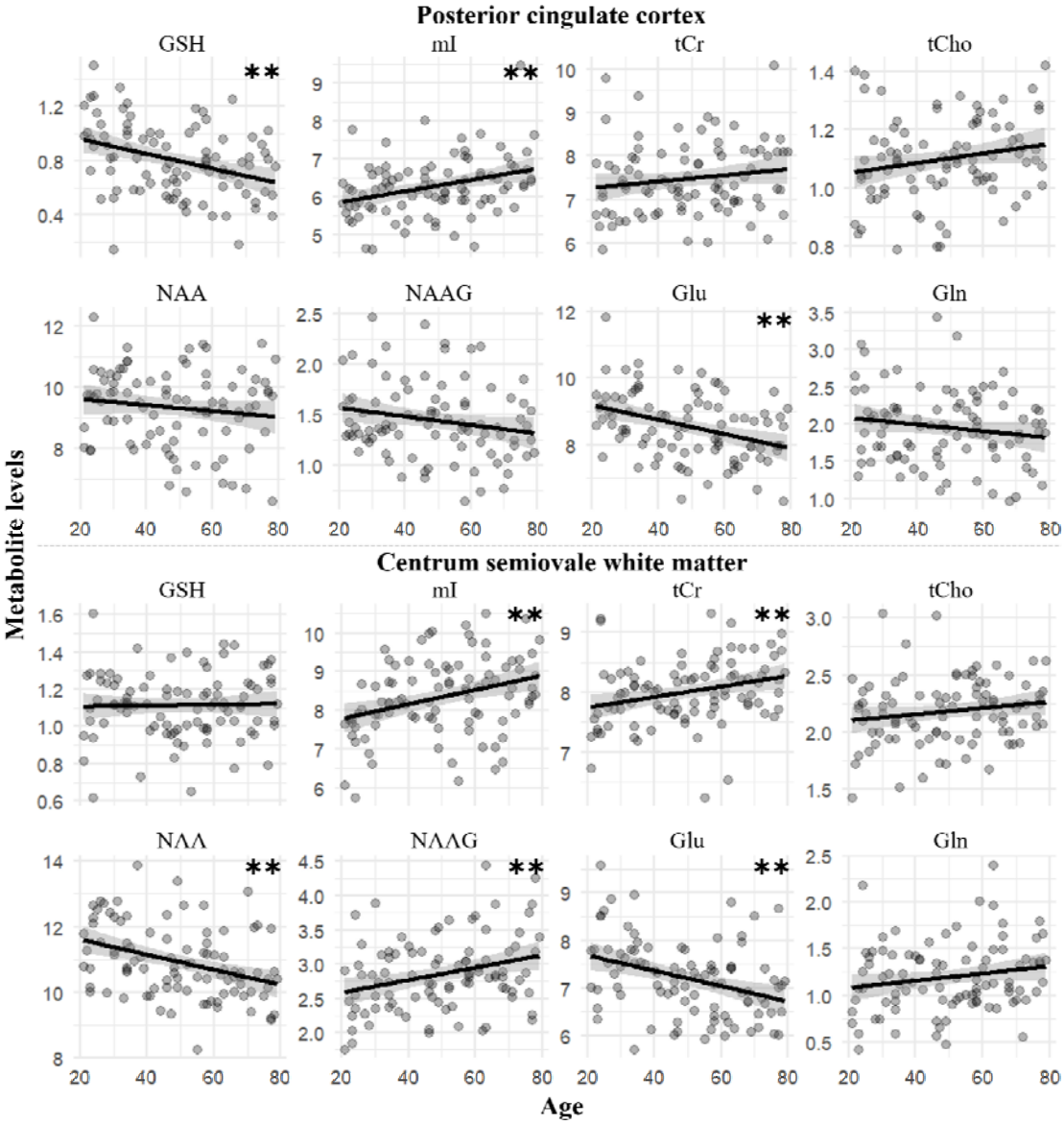

Figure 2. Age-specific metabolite level changes with age as a continuum.

Abbreviations: **, $p < 0.01$; Gln, glutamine; Glu, glutamate; GSH, glutathione; mI, *myo*-inositol; NAA, *N*-acetylaspartate; NAAG, *N*-acetylaspartyl-glutamate; tCho, total choline; tCr, total creatine.

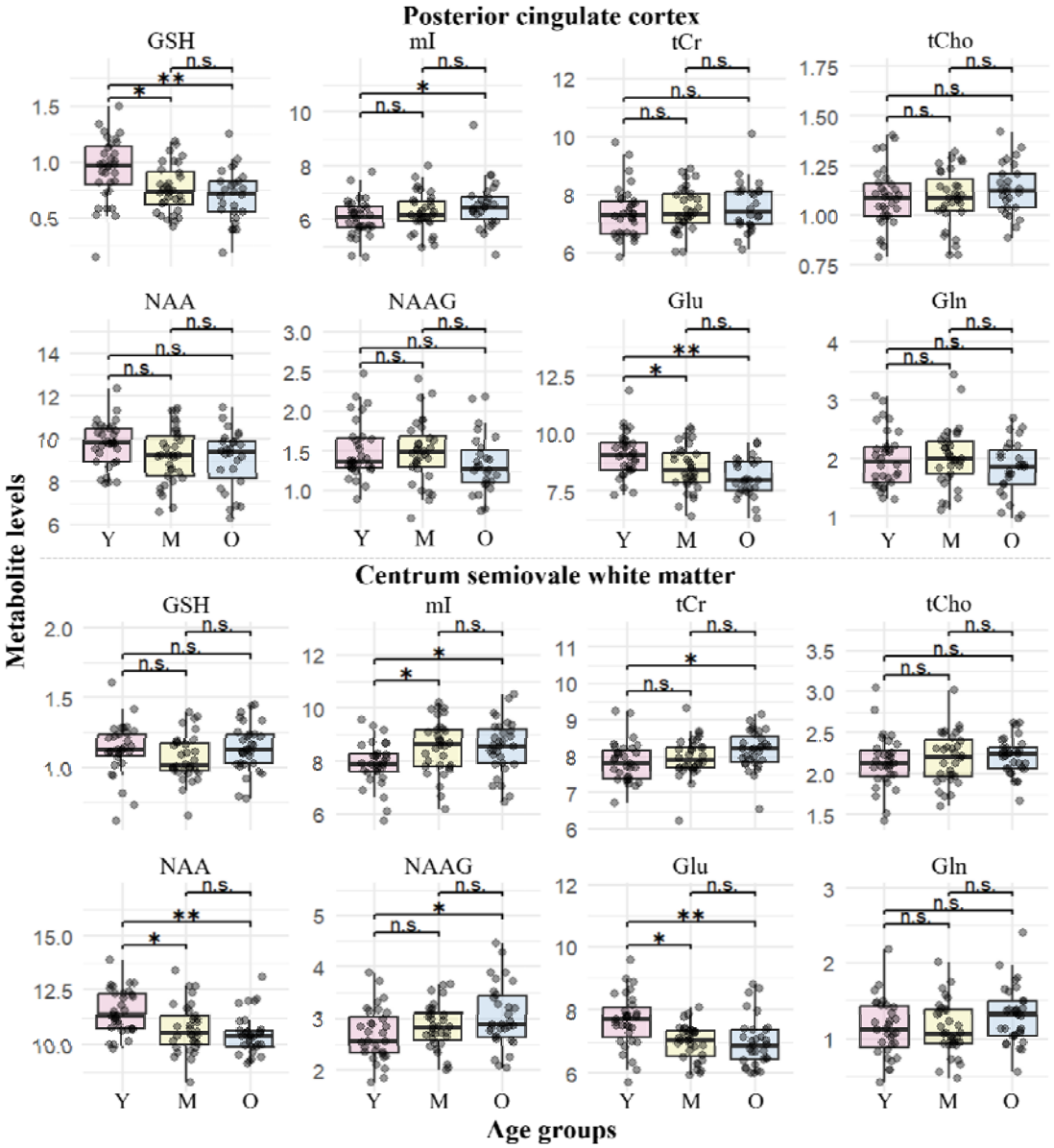

Figure 3. Age-specific metabolite level changes between age groups.

Abbreviations: *, $p < 0.05$; **, $p < 0.01$; Gln, glutamine; Glu, glutamate; GSH, glutathione; M, middle-aged; mI, *myo*-inositol; NAA, *N*-acetylaspartate; NAAG, *N*-acetylaspartyl-glutamate; n.s., not significant; O, older; tCho, total choline; tCr, total creatine; Y, younger.

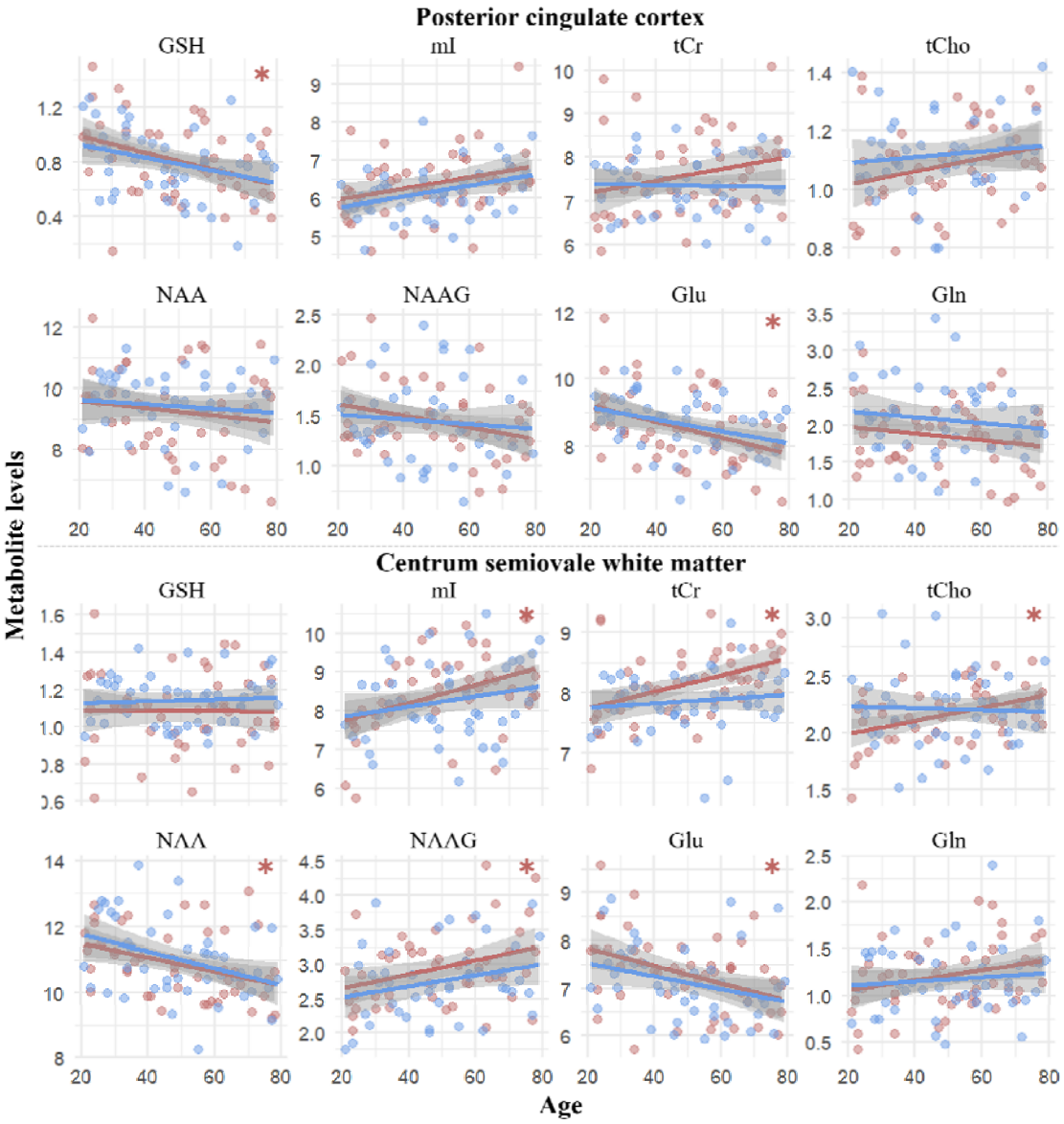

Figure 4. Sex-specific metabolite level changes with increasing age. Brown represents women and blue represents men.

Abbreviations: *, $p < 0.05$; Gln, glutamine; Glu, glutamate; GSH, glutathione; mI, *myo*-inositol; NAA, *N*-acetylaspartate; NAAG, *N*-acetylaspartyl-glutamate; tCho, total choline; tCr, total creatine.

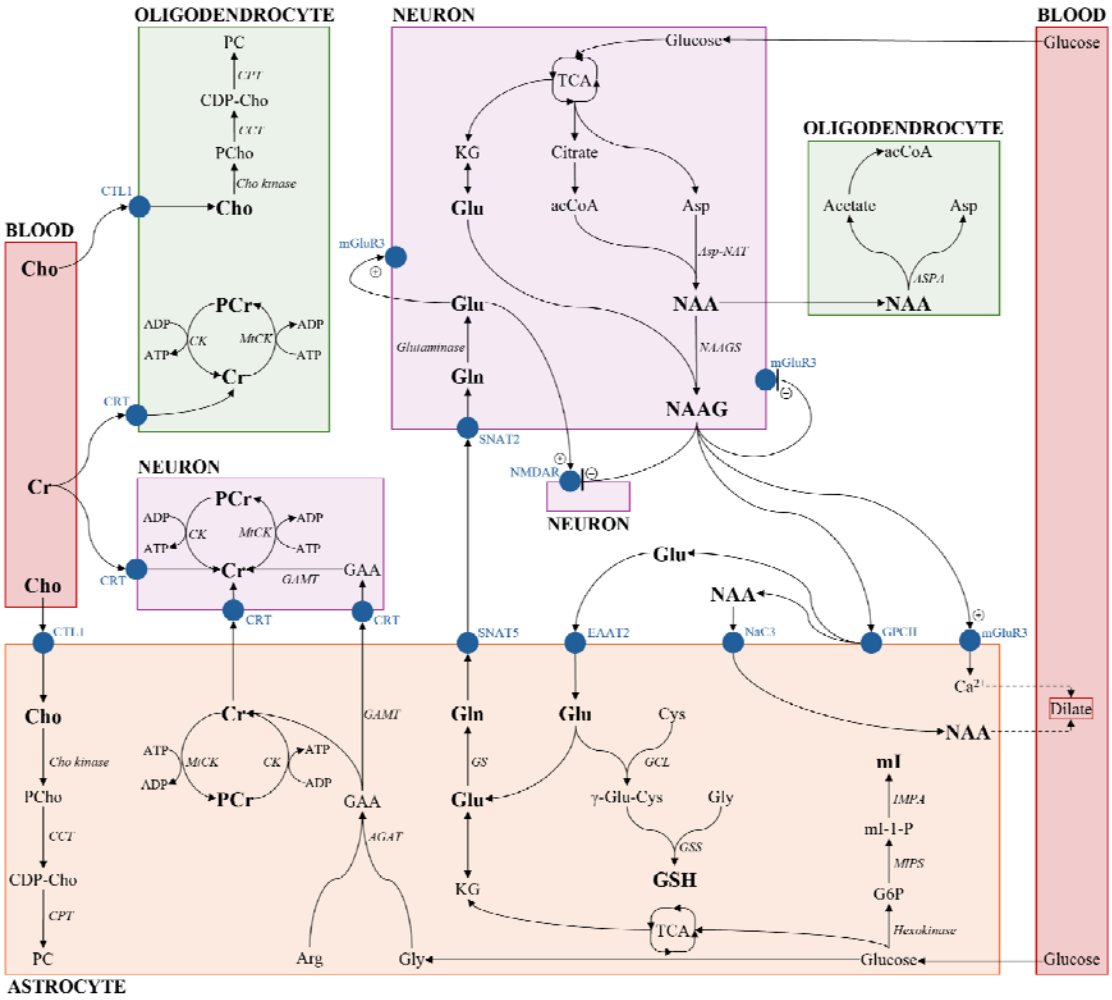

Figure 5. Depiction of metabolic pathways in different brain cell types. Our MRS-detected metabolites are in bold. Enzymes are in italics. Transporters and receptors are in blue.

Abbreviations: +, stimulation; -, inhibition; acCoA, acetyl coA; AGAT, arginine-glycine amidinotransferase; Arg, arginine; Asp, aspartate; Asp-NAT, aspartate N-acetyltransferase; ASPA, aspartoacylase; ADP, adenosine diphosphate; ATP, adenosine triphosphate; Ca^{2+}, calcium; CCT, phosphocholine cytidylyltransferase; CDP-Cho, cytidine diphosphate-choline; Cho, choline; CK, creatine kinase; CPT, cholinephosphotransferase; Cr, creatine; CRT, creatine transporter; CTL1, choline transporter-like 1 protein; Cys, cysteine; EAAT2, excitatory amino acid transporter 2; G6P, glucose-6-phosphate; GAA, guanidinoacetate; GAMT, guanidinoacetate methyltransferase; GCL, glutamate-cysteine ligase; Gln, glutamine;

Glu, glutamate; GPCII, glutamate carboxypeptidate II receptor; GSH, glutathione; GS, glutamine synthetase; GSS, glutathione synthetase; Gly, glycine; γ-Glu-Cys, gamma-glutamate-cysteine; IMPA, inositol monophosphate; KG, α-ketoglutarate; mGluR3, metabotropic Glu receptor 3; mI, *myo*-inositol; mI-1-P, myo-inositol-1-phosphate; MIPS, mI phosphate synthase; mtCK, mitochondrial CK; NAA, *N*-acetylaspartate; NAAG, *N*-acetylaspartyl-glutamate; NAAGS, NAAG synthase; NMDAR, *N*-methyl-D-aspartate receptor; PC, phosphatidylcholine; PCr, phosphocreatine; PCho, phosphocholine; SNAT2, amino acid transporter 2; SNAT5, amino acid transporter 5; TCA, tricarboxylic acid cycle.

TABLE LEGENDS

Table 1. Participant demographics.

Abbreviations: BMI, body-mass index = weight (kg) / [height (m)] ^{2}; SD, standard deviation.

	Younger (20-39 years)	**Middle-aged** (40-59 years)	**Older** (60-79 years)
N (women)	32 (16)	32 (16)	31 (16)
Age (mean ± SD)	29.25 ± 5.34	50.58 ± 5.86	69.48 ± 6.02
BMI (mean ± SD)	25.89 ± 6.43	27.99 ± 5.61	27.27 ± 10.31
Education (years)	18.05 ± 2.04	16.05 ± 2.51	16.26 ± 2.51
Symbol digit modalities test	65.31 ± 8.77	55.45 ± 8.58	43.00 ± 7.96
9-hole peg test	18.81 ± 2.09	20.08 ± 2.69	21.61 ± 2.62
Timed 25-foot walk test	3.82 ± 0.57	4.05 ± 0.96	4.36 ± 1.02

Table 2. Metabolite levels per region of interest, and statistical significance with age (continuum and groups) and sex.

Abbreviations: [a], significant association with age as a continuum; [b], significant association with age as a continuum in women only; [c], significant group differences relative to younger adults; CSWM, centrum semiovale white matter; [d], significant group differences relative to younger adults in women only; Gln, glutamine; Glu, glutamate; GSH, glutathione; *italics*, borderline significance; mI, *myo*-inositol; NAA, *N*-acetylaspartate; NAAG, *N*-acetylaspartyl-glutamate; PCC, posterior cingulate cortex; tCho, total choline; tCr, total creatine.

Metabolite, Age group	PCC (mean ± SD)	CSWM (mean ± SD)
GSH		
Age (continuum)	0.804 ± 0.264 [a, b]	1.113 ± 0.176
Younger	0.934 ± 0.285	1.131 ± 0.190
Middle-aged	0.760 ± 0.212 [c]	1.070 ± 0.166
Older	0.699 ± 0.237 [c, d]	1.140 ± 0.168
mI		
Age (continuum)	6.265 ± 0.784 [a]	8.336 ± 0.990 [a, b]
Younger	6.049 ± 0.689	7.907 ± 0.848
Middle-aged	6.259 ± 0.718	8.556 ± 1.004 [c, d]
Older	6.538 ± 0.907 [c]	8.539 ± 0.996 [c, d]
tCr		
Age (continuum)	7.475 ± 0.825	8.003 ± 0.552 [a, b]
Younger	7.380 ± 0.886	7.855 ± 0.559
Middle-aged	7.480 ± 0.742	7.975 ± 0.538
Older	7.586 ± 0.863	8.180 ± 0.526 [c, d]
tCho		
Age (continuum)	1.099 ± 0.143	2.183 ± 0.289 [b]
Younger	1.086 ± 0.151	2.145 ± 0.327
Middle-aged	1.084 ± 0.145	2.190 ± 0.311
Older	1.132 ± 0.130	2.213 ± 0.222 [*d*]
NAA		
Age (continuum)	9.346 ± 1.273	10.924 ± 1.094 [a, b]
Younger	9.749 ± 1.056	11.527 ± 0.517
Middle-aged	9.184 ± 1.315	10.744 ± 1.110 [c]
Older	9.051 ± 1.381	10.507 ± 0.920 [c, d]
NAAG		

	Age (continuum)	1.448 ± 0.378	2.855 ± 0.537 [a, b]
	Younger	1.499 ± 0.358	2.686 ± 0.517
	Middle-aged	1.488 ± 0.393	2.839 ± 0.433
	Older	1.338 ± 0.373	3.042 ± 0.607 [c]
Glu			
	Age (continuum)	8.570 ± 1.011 [a, b]	7.209 ± 0.794 [a, b]
	Younger	9.071 ± 0.959	7.654 ± 0.846
	Middle-aged	8.479 ± 0.977 [c]	6.989 ± 0.555 [c]
	Older	8.065 ± 0.846 [c, d]	6.989 ± 0.783 [c, d]
Gln			
	Age (continuum)	1.954 ± 0.494	1.193 ± 0.374
	Younger	1.992 ± 0.486	1.136 ± 0.377
	Middle-aged	2.020 ± 0.513	1.136 ± 0.350
	Older	1.827 ± 0.475	1.309 ± 0.378